5th International Symposium on Three-Dimensional Electromagnetics
Sapporo, Japan, May 7–9, 2013

# Enhancing Resolution of 3D-EM Inversion Models through a Co-operative Approach

Michael S.G. McMillan[1], and Douglas W. Oldenburg[1]
[1]University of British Columbia, Geophysical Inversion Facility. Vancouver, B.C., Canada

## SUMMARY

We present a method for co-operatively using multiple electromagnetic (EM) datasets to produce a consistent three-dimensional resistivity inversion model with improved resolution. Both field data from the Antonio gold deposit in Peru, and synthetic data are used to demonstrate this technique. We first separately invert airborne time-domain EM (AEM), controlled source audio-frequency magnetotellurics (CSAMT) and time-domain pole-dipole direct current resistivity (DC) field measurements to recover 3D resistivity models. Each inversion recovers a large resistor related to gold hosted silica alteration. Collectively they map a resistor location that is in reasonable agreement with its known outline, as drawn from geologic drill logs. Variations between the 3D models exist, and this motivates a subsequent co-operative method in which the AEM resistivity model is used as a reference model for a joint inversion of the CSAMT and DC data. The 3D co-operative result appears to define the target resistor with greater precision than the individual inversions, and additionally it highlights small conductive zones of potential interest within the resistive region. Synthetic modeling of the same three data sets over a simulated resistivity distribution further demonstrates that the co-operative approach qualitatively and quantitatively improves the accuracy of the resulting inversion model in the target area.

**Keywords:** co-operative inversion, forward modeling, airborne-EM, CSAMT, DC resistivity

## INTRODUCTION

Electromagnetics (EM) is an important tool in many areas of research and industry, and specifically in mineral exploration because it provides a platform to image three-dimensional (3D) electrical resistivity distributions in the sub-surface of the earth. Electrical resistivity measures the degree to which a material opposes the flow of electric current, and this physical property can help distinguish rock types and alteration zones due to resistivity contrasts with background lithologies. For this reason, multiple EM datasets are often acquired over a common area of interest, and conventionally each dataset is used separately to produce a three-dimensional resistivity inversion model. This abstract focuses on inverting field and synthetic data from individual surveys, and then unifying the models by using a co-operative procedure.

In this study, three EM datasets are presented: airborne time-domain EM (AEM), controlled source audio-frequency magnetotellurics (CSAMT) and direct current resitivity (DC). Field data, courtesy of Newmont Mining Corporation, comes from the Antonio gold deposit, which is located within the larger world-class Yanacocha high sulfidation epithermal gold system, in Peru. The majority of gold mineralization at Antonio resides within highly resistive envelopes of silica alteration, which are applicable targets for EM surveys (Teal & Benavides, 2011). When multiple datasets exist over a common area, such as Antonio, it is important to invert each one individually in 3D to estimate a resistivity structure sensitive to that particular survey. Discrepancies between spatially coincident models naturally occur due to numerous causes: data quality variations between surveys, acquisition location differences, and modeling errors etc. When contrasting results are encountered, traditionally each field inversion model is evaluated to decide which one is the most trustworthy. This highlights the need for a co-operative technique, where multiple EM datasets can work together to generate one consistent 3D physical property model. Research from this abstract builds upon previous work on geophysics data at the Antonio gold deposit by (Oldenburg et al., 2004) and (McMillan & Oldenburg, 2012).

## INDIVIDUAL FIELD INVERSIONS

### Airborne time-domain EM

A helicopter based airborne time-domain EM survey was collected over the Antonio deposit area using a Newmont Mining Corporation internally developed and operated EM system, NEWTEM (Eaton et al., 2002). Five lines were flown in an East-West orientation over the primary area of interest with a peak current of 275 amps, a transmitter loop dipole moment of 80,000 $Am^2$, and $\frac{dBz}{dt}$ secondary responses measured 30 - 2000 micro-seconds after current shut-off. Line spacings for the survey were 200m, with a station spacing of 20m yielding 268 total transmitter locations. The data were inverted and Figure 1a shows a constant elevation slice (3870m above sea level) through the ensuing 3D inversion model along with data locations. The result agrees well with the resistive silica alteration

outline mapped by drilling (dashed red line), although the southern portion of the resistor is not captured. Despite rolling topography, a constant elevation slice of 3870m corresponds to an average depth below surface of roughly 75m, although it ranges from 10m - 150m throughout the survey area. Inversion errors of 10% plus a 30 uV noise floor were assigned using a 25m x 50m x 25m core mesh.

### CSAMT

An asynchronous scalar CSAMT survey was acquired by Quantec Geoscience with a total of five East-West (EW) and eight North-South (NS) lines. Two transmitters sites existed: an EW oriented transmitter to the South for EW lines, and a NS oriented transmitter to the East for NS lines. This permitted the earth to be energized from two orthogonal directions. Line spacings varied between 150-200m, and stations were spread 50m apart. Data from 11 frequencies ranging between 2Hz - 2048Hz were subsequently inverted. Figure 1b portrays a 3870m constant elevation result, which once again matches nicely with the dashed red silica alteration outline. The recovered resistivity magnitudes compare well with the AEM outcome, however there are differences in resistivity geometries between the images, especially in the central and southern portions. Inversion error assignments of 15% plus a 3.5e-8 V/m noise floor (Electric Field), and 15% plus a 2.7e-8 A/m noise floor (Magnetic Field) were applied on a 25m x 50m x 25m core mesh.

### DC resistivity

A conventional in-line time-domain pole-dipole DC Resistivity survey with six East-West lines spread 50-200m apart with a mix of 50m and 150m dipoles was also gathered by Newmont Mining Corporation. Potential differences were inverted to produce a 3870m elevation slice shown in Figure 1c along with receiver dipoles locations. Resistivity magnitudes align well with AEM and CSAMT results in the northern region, although the southern zone is contrarily mapped as conductive. Similarly the recovered model matches the alteration outline in the North quite closely but not in the South. Inversion errors of 5% plus a 1.2 mV noise floor were applied on a 15m x 50m x 15m core mesh.

Of note, the resistivity colour scale is consistent across all field inversions in Figure 1, as is the reference model used: a 50 Ohm-m half-space. Additionally all inversions in this study used adaptive mesh software from University of British Columbia Geophysical Inversion Facility, (Oldenburg & Li, 1994), (Haber, Oldenburg, & Shehktman, 2007). Error noise floors for all data sets were chosen as two standard deviations below the logarithmic mean of the data, while the error percentages were picked with regards to noisiness and reliability of the data.

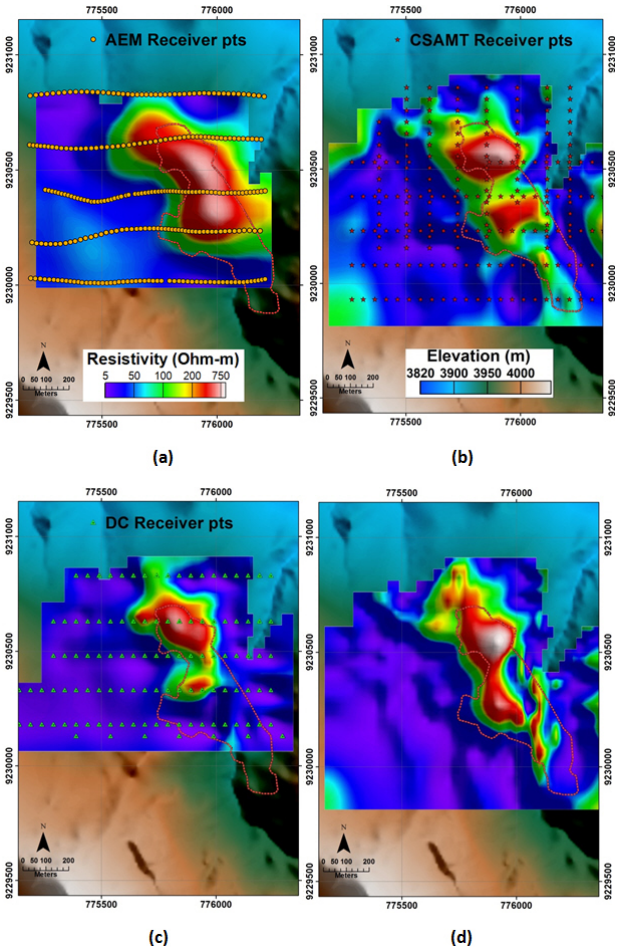


**Figure 1.** Field 3D inversions. 3870m elevation slice overlaid on topography. Resistor outline from drilling in dashed red. a) AEM, b) CSAMT, c) DC Resistivity, d) Co-operative CSAMT/DC inversion with AEM reference model.

## CO-OPERATIVE FIELD INVERSION

There are numerous ways in which multiple EM datasets can be input into a single inversion modeling program. Our approach is to treat DC data as a low frequency CSAMT input, and invert both datasets simultaneously. Since CSAMT measurements are complex values (both real and imaginary components), DC voltages are converted into real electric-fields (E-fields) by dividing by the dipole length, while the imaginary E-fields are set to zero. This approximation holds for low frequencies in areas that are not highly conductive. The validity of this approximation can be checked by carrying out a 3D forward modeling to compute the complex responses at a low frequency and ensuring that the imaginary E-fields are below the noise floor level. In the case of Antonio, an 8-second transmitter pulse was used to collect DC field data, which corresponds to a frequency of 0.125Hz. Subsequent forward modeling at 0.125Hz using the DC resistivity inversion model produced imaginary E-fields with

an average magnitude of 1.5e-7 V/m, well below the noise floor of 2.4e-5 V/m (1.2mV). As such this approximation was deemed valid for this area. The inversion of a merged CSAMT and DC dataset then produced a co-operative model, using the AEM result from Figure 1a as a reference model, and a 3870m constant elevation image through this outcome is shown in Figure 1d. Inversion error levels were kept identical to those from the CSAMT trial except for the addition of a noise floor of 2.4e-5 V/m for 0.125Hz DC derived E-fields. The recovered resistor in Figure 1d agrees well with drilling inferred information, while additional conductive features within the resistor also emerge. These small conductive zones can potentially be representative of clay and highly mineralized areas of interest. Because an exact resistivity distribution is not known, it is impossible to evaluate the precise accuracy of each recovered model. However, the co-operative result provides a unified model which accurately defines the resistor outline, and potentially images conductive features related to mineralization within the target area.

## SYNTHETIC INVERSION MODELING

Synthetic inversion modeling involves solving the forward problem over a pre-defined resistivity distribution, and then attempting to recover the original model. Since a true answer is known, it becomes possible to evaluate resulting outcomes with confidence. To maintain consistency with field datasets, the synthetic model was designed to encapsulate primary features of the Antonio area. Therefore, a 225m thick 1000 Ohm-m resistor was placed in a uniform 50 Ohm-m background with two embedded conductive 10 Ohm-m blocks of dimensions: 100m x 150m x 100m. Figure 2a portrays a 3870m constant elevation slice through the model. Topography over Antonio was also kept for the synthetic study as shown in Figure 2b. Although equivalent in size, the northern conductive block was buried at a depth of 75m while the southern anomaly was exposed at surface. Forward modeling of AEM, CSAMT and DC surveys were carried out keeping data locations and other specifications equivalent to field setups. With Gaussian noise added, each forward modeled dataset was inverted in 3D on a 25m x 50m x 25m core mesh with matching inversion errors to field counterparts. Fixed elevation slices at 3870m through ensuing AEM, CSAMT and DC inversions appear in Figures 3a, 3b and 3c respectively. The images all display a resistive body centered in the correct location, but variations between the three recoveries are noticeable. In Figure 3a, AEM flight line locations bypass the southern conductor, and likewise the inversion only detects a subtle anomaly. Moreover, the buried northern conductor is not imaged even though several data points are collected directly over the block. Figure 3b demonstrates that the CSAMT recovery detects the southern conductor, as well as a faint hint of the northern block. A slight overall magnitude decrease of the large resistor in comparison to AEM is noted, in addition to an improved detection of the southernmost resistive zone, which coincides with the bottom CSAMT line.

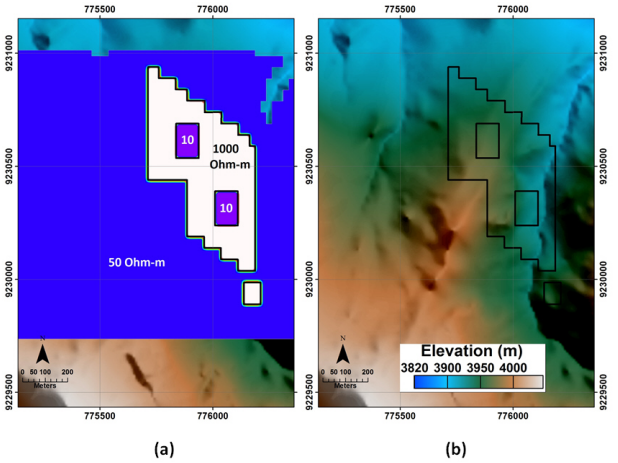


**Figure 2.** Synthetic true model. a) 3870m elevation resistivity slice. b) topography with resistor outline.

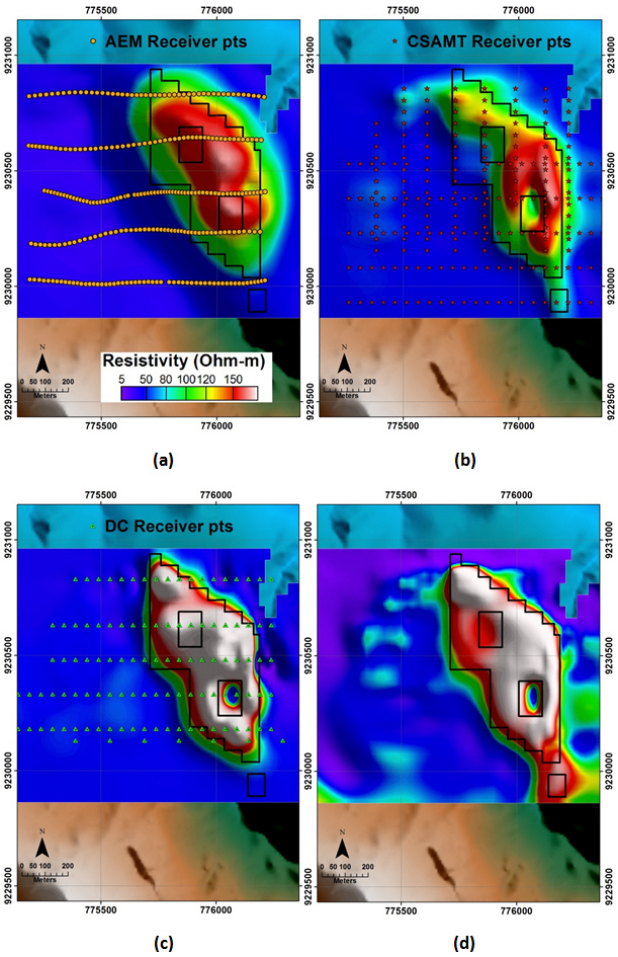


**Figure 3.** Synthetic 3D inversions, 3870m elevation slice, overlaid on topography. Resistor outline in black. a) AEM, b) CSAMT, c) DC Resistivity, d) Co-operative CSAMT/DC with AEM reference model.

In Figure 3c, the DC recovery depicts the overall magnitude and geometry of the resistor and southern conductive block quite nicely. Resistivity magnitudes are closer to the synthetic model compared to CSAMT and AEM results, although no recovery of the northern block is seen. Finally Figure 3d shows a co-operative inversion result using CSAMT and DC data simultaneously with an AEM reference model. The resistor magnitude is imaged more uniformly, the southern conductor is located and the northern anomaly is now faintly detected. Some minor erroneous structure does emerge in the background region of Figure 3d away from the region of interest.

We now have four resistivity models and to help assess how well each inversion has done in recovering information about our target resistive zone, we evaluate a residual (R) defined as:

$$R = \frac{1}{N}\|\log(m) - \log(m_t)\|_2^2 \quad (1)$$

In Equation 1 $(m)$ and $(m_t)$ are the recovered and true resistivity values respectively, $N$ is the total number of cells within the resistive zone (including the two conductive regions) and $\| \ \|_2^2$ is the squared $\ell^2$ norm. A reduced R value refers to a smaller deviation from the true model, and hence a more accurate recovery. The residuals are shown in Table 1 for the four synthetic inversions as well as for a 50 Ohm-m half-space. The table shows that the co-operative inversion performs the best, followed closely by the DC result, while the AEM and CSAMT models fared worse. Not surprisingly, all four inversions recover a more accurate model compared to a uniform background half-space. This synthetic example demonstrates that a co-operative 3D inversion that successfully includes all the geophysical data into one consistent model can improve the accuracy of the recovered anomalies. Because of its close association with the field data example, we anticipate that the same conclusion can be applied there.

**Table 1.** Calculated residual of synthetic inversions.

| | Residual (R) |
|---|---|
| 50 Ohm-m half-space | 1.62. |
| AEM | 1.05. |
| CSAMT | 1.08. |
| DC | 0.59. |
| Co-operative | 0.52. |

## CONCLUSIONS AND FUTURE WORK

In this study, three spatially coincident EM datasets were inverted in 3D using both field data at the Antonio gold deposit, as well as synthetic data. Individual field inversion models outlined a resistor of approximately equal magnitude, whose outline collectively agreed well with geologic drill logs. Some resistivity variations occurred between the three outputs, and these were reconciled by using a co-operative inversion method. This technique incorporated DC resistivity data as low frequency CSAMT data, and simultaneously used both datasets, along with an AEM resistivity reference model, in the inversion. The co-operative result matched well with the known resistor outline, and appeared to be a qualitative improvement over inversion models created using single EM datasets alone. In synthetic modeling tests, all simulated datasets recovered the target resistor, but only the CSAMT and DC data were sensitive to the southern conductor. A co-operative inversion not only recovered a consistent resistor magnitude and the southern conductive anomaly, but also faintly imaged the northern conductor, which no other dataset was able to delineate with distinction. The co-operative model also quantitatively had the most accurate recovery of the entire target region by having the lowest residual (R). Future research aims at further investigating strategies for co-operative inversion that increase the fidelity of the final outcome.

## ACKNOWLEDGMENTS

The authors thank Newmont Mining Corporation for permission to utilize and show the data at Antonio.

## REFERENCES

Eaton, P., Anderson, B., Nilsson, B., Lauritsen, E., Queen, S., & Barnett, C. (2002). Newtem - a novel time-domain helicopter electromagnetic system for resistivity mapping. *72nd Annual International Meeting, SEG, Expanded Abstracts*, *21*, 1-4.

Haber, E., Oldenburg, D. W., & Shehktman, R. (2007). Inversion of time domain three-dimensional electromagnetic data. *Geophysical Journal International*, *171*, 550-564.

McMillan, M., & Oldenburg, D. W. (2012). Three-dimensional electromagnetic and electrical inversions over the antonio gold deposit in peru. *82nd Annual International Meeting, SEG, Expanded Abstracts*, *31*, 1316-1320.

Oldenburg, D. W., & Li, Y. (1994). Inversion of induced polarization data. *Geophysics*, *59*, 1327-1341.

Oldenburg, D. W., Shehktman, R., Eso, R. A., Farquharson, C. G., Eaton, P., Anderson, B., et al. (2004). Closing the gap between research and practice in em data interpretation. *74th Annual International Meeting, SEG, Expanded Abstracts*, *23*, 1179-1182.

Teal, L., & Benavides, A. (2011). History and geologic overview of the yanacocha mining district, cajamarca, peru. *Economic Geology*, *105*, 1173-1190.